Oxadiazole derivatives as stable anolytes for >3 V non-aqueous redox flow battery

Jesse, Kate Ashley
Diaz Abad, Sergio
Van Pelt, Christopher Evan
Pentzer, Emily
Davis, Benjamin L.
Maurya, Sandipkumar

To be published in: Chemical Engineering Journal

DOI to publisher's version: 10.1016/j.cej.2024.153732

Journal Pre-proofs

Oxadiazole derivatives as stable anolytes for >3 V non-aqueous redox flow battery

Kate A. Jesse, Sergio Diaz Abad, Christopher E. Van Pelt, Emily Pentzer, Benjamin L. Davis, Sandip Maurya

PII: S1385-8947(24)05221-5
DOI: https://doi.org/10.1016/j.cej.2024.153732
Reference: CEJ 153732

To appear in: *Chemical Engineering Journal*

Received Date: 26 March 2024
Revised Date: 6 June 2024
Accepted Date: 3 July 2024

Please cite this article as: K.A. Jesse, S. Diaz Abad, C.E. Van Pelt, E. Pentzer, B.L. Davis, S. Maurya, Oxadiazole derivatives as stable anolytes for >3 V non-aqueous redox flow battery, *Chemical Engineering Journal* (2024), doi: https://doi.org/10.1016/j.cej.2024.153732

Oxadiazole Derivatives as Stable Anolytes for >3 V Non-Aqueous Redox Flow Battery

Kate A. Jesse,[a] Sergio Diaz Abad, [a] Christopher E. Van Pelt,[b] Emily Pentzer,[b] Benjamin L. Davis, [a] and Sandip Maurya [a]**

[a]MPA-11: Materials Physics Applications, Los Alamos National Laboratory, Los Alamos, NM, 87545, USA

*Email: smaurya@lanl.gov, bldavis@lanl.gov

[b]Department of Materials Science & Engineering, Texas A&M University, College Station, Texas 77843

KEYWORDS

Non-Aqueous Redox Flow Battery; Energy Storage; Organic Charge Carrier; Anolyte

ABSTRACT.

Effective utilization of energy from renewable sources such as wind and solar requires the development of long duration energy storage (LDES) systems that can accommodate intermittent energy accrual. One option under investigation is the use of a redox flow battery (RFB). A significant amount of work has explored aqueous RFB systems with a variety of inorganic and organic carriers. However, moving to a nonaqueous solvent such as acetonitrile (MeCN) for RFB provides a much larger electrochemical window, which could lead to increased energy density if properly utilized. In this work, we investigate a series of 2,5-diphenyl-1,3,4-oxadiazole (DiPhenOx) derivatives as anolytes for a redox flow battery. DiPhenOx has a low voltage redox event that, while reversible by cyclic voltammetry, was determined to be irreversible during bulk electrolysis. To improve cycling performance, we introduced various ester and cyano groups to the phenyl rings of DiPhenOx using molecular engineering. We characterized these derivatives spectroscopically and electrochemically to assess their feasibility for flow battery applications. The ester derivatives with the best cycling performance were tested in a flow cell vs. ferrocene, 2,5-di-tert-butyl-1,4-bis(2-methoxyethoxy)benzene (DBBB) and thianthrene, which resulted in ~2 V, ~3 V and ~3 V redox flow batteries, respectively.

INTRODUCTION

Recent years have seen a growth in the use of renewable energy sources such as wind and solar.[1,2] However, to use these intermittent energy sources more effectively, appropriate energy storage technologies must be in place. In particular, LDES technologies are needed as evidenced by the US DOE Grand Challenge.[3] While Li-ion batteries are by far the most well investigated, they are best suited for short and medium duration energy storage, and cost is still limiting deployment.[4] Efforts have been made in the area of pumped hydro, which is the least expensive technology energy storage technology available in the United States.[5–7] However, pumped storage hydropower has severe limitations due to topological requirements and building costs which have stifled universal deployment of this technology.[8–10] Another option under investigation for LDES are RFBs.[11,12] Non hybrid RFBs allow for the storage of energy in various redox states of a molecule or polymer. These chemical species are stored in tanks, which are separate from the cell that facilitates power.[12] This allows power and energy to be scaled individually for any given application.

Significant research into aqueous RFBs has been done with both organic and inorganic carriers.[13] Carriers such as $V(acac)_3$,[14–18] Fe chelates,[19–26] anthraquinone based molecules,[27–33] and fluorenone based molecules[34,35] have been particularly promising. Many of these RFBs utilize aqueous systems to capitalize on the cost effectiveness and environmentally benign properties of water. However, the electrochemical stability window of water is relatively small, often being cited as ~1.23 V, though windows of up to 1.7 V are accessible if Pt electrodes are avoided.[13] In contrast, nonaqueous solvents often have an electrochemical window exceeding 4 V.[36–38] Since the energy stored in a RFB is directly related to the difference in voltage between the catholyte and anolyte, having a larger solvent window opens the possibility of building a battery with a higher energy storage capacity.[12] A variety of metal complexes, featuring Fe, Ni, Zn, Cr, and Mn among others, have been investigated as carriers for NRFBs.[26,39–43] However, due to the high cost of many of these metals and limited solubility and chemical stability in charged states in many cases, researchers have turned

to organic compounds when looking for appropriate catholytes and anolytes.[44,45] A goal of our research is to develop a charge carrier which could enable a >3 V Non-aqueous redox flow battery (NRFB) that takes advantage of the larger electrochemical stability window of non-aqueous solvents.

The compound 2,5-diphenyl-1,3,4-oxadiazole (DiPhenOx) could be a promising anolyte carrier for a NRFB for a variety of reasons. First, it has good solubility in acetonitrile (MeCN) at 240(30) mM in pure MeCN without modification. Additionally, it exhibits a reductive wave at -2.46 V vs Ag/Ag^+ in MeCN that is reversible when analyzed by cyclic voltammetry (CV). Herein we report modification of the parent DiPhenOx, which was undertaken to improve its durability for charge/discharge cycling. The modified compounds were then paired with an appropriate catholytes to form a ~2 V or ~3 V NRFB. Additionally, the effect of these modifications on the solubility of the molecules was investigated.

RESULTS AND DISCUSSION

Electrochemical characterization of DiPhenOx

Previous studies focused on chemiluminescence collected CV data on DiPhenOx.[46] We were able to reproduce these data and observe a reversible reduction event at -2.46 V vs Ag/Ag^+ for DiPhenOx in MeCN. This is an extremely low potential to observe a reversible reduction event compared to other known organic anolytes.[47] As such, DiPhenOx piqued our interest as a possible anolyte for RFB applications. The CV data for this reduction has a current ratio of i_c/i_a = 0.92, which quantitatively supports that this reduction as reversible. However, when bulk cycled in a symmetric H-cell, DiPhenOx showed a rapid decline in the utilization (electrons/molecule) and in the coulombic efficiency within just a few charge/discharge cycles (Figure 3 and S 26), indicating chemical degradation. Specifically, a coulombic efficiency of ~20% and greater than 80% loss in utilization for both the charge and discharge cycling was observed after 25 cycles. As such, DiPhenOx is not a suitable anolyte for NRFB applications. However, we hypothesized that with appropriate modifications, DiPhenOx could be stabilized to increase its durability to cycling, and effectively utilized as an anolyte in a NRFB.

Synthesis of DiPhenOx derivatives

Stabilization of carriers in redox flow batteries can be achieved in a variety of ways. One strategy is to extend the aromatic system in such a way as to stabilize the radical anion or cation. Alternatively, the addition of electron withdrawing groups (EWG's) or electron donating groups (EDG's) can be used to shift the potential of the reduction event to higher or lower potential.[42,48] In this case, lessening the reduction potential of the anolyte by stabilizing the negative charge with proximal EWGs should result in a more stable radical anion.[49] We decided to use this strategy, and add EWG's in the form of –CN or –(C=O)OR in the *para* position of the phenyl ring within the compound. This modification extends the aromatic system by 2 or 3 atoms respectively and introduces an electron EWG via resonance effects. 2,5-di(4-cyanophenyl)-1,3,4-oxadiazole (**1**) is synthesized using an Ullman reaction between the aryl bromides of the 2,5-di(4-bromophenyl)-

1,3,4-oxadiazole and Cu(CN) salt (Figure 1, Scheme S1).[50] The ester derivatives (**2** and **3**) were prepared by oxidizing 2,5-di(4-methylphenyl)-1,3,4-oxadiazole with potassium permanganate, forming the acid chloride, then reacting with an appropriate alcohol (Figure 1, Scheme S2). Ethanol was chosen due to its wide availability and 2-methoxyethanol was selected in an effort to increase the overall solubility of the final molecule, **3**, via the addition of an ether group. The incorporation of ether moieties, specifically polyethyleneglycol (PEG), has been shown to enhance solubility in other organic systems in MeCN.[28,39,51–57] The identity and purity of the three compounds were characterized by ^{1}H and ^{13}C nuclear magnetic resonance (NMR) and infrared (IR) spectroscopy. The expected peak patterns were observed by NMR spectroscopy. Similarly, the characteristic C≡N and ester C=O stretches were observed by IR spectroscopy (Figures S1-S9).

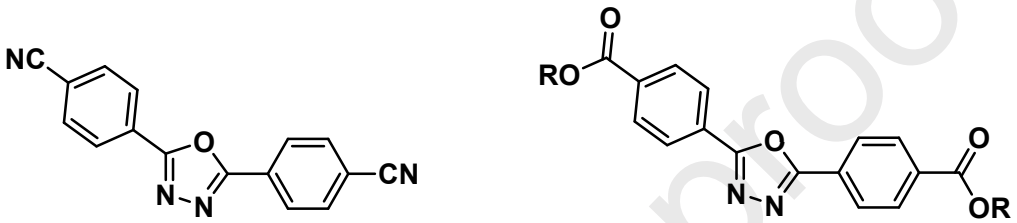

Figure 1. Derivatives of DiPhenOx synthesized for electrochemical testing.

*Cyclic voltammetry of **1**, **2**, and **3***

Unlike the parent DiPhenOx, **1**, **2**, and **3** all exhibit two reduction events (Table 1, Figure 2). For all three, the first reduction (x) is reversible by CV with $i_c/i_a = 1\pm0.08$, where a value of 1 ± 0.1 would correspond to a reversible redox event. By the same criteria, the second reduction (y) for **1** and **3** is also reversible (Table 1). Compound **2**'s second reduction wave has a current ratio of 0.89, right on the cusp of what is considered reversible. The potentials of these negative waves are both positively shifted, as expected with the addition of EWG's. Interestingly, the second reduction (y) events for **2** and **3** occur at essentially identical potentials, suggesting this wave is physical isolated or without resonance communication to the ether functionality. As such, the effect of the ether moieties on solubility can be isolated from their effect on reduction potentials in **2** and **3**.

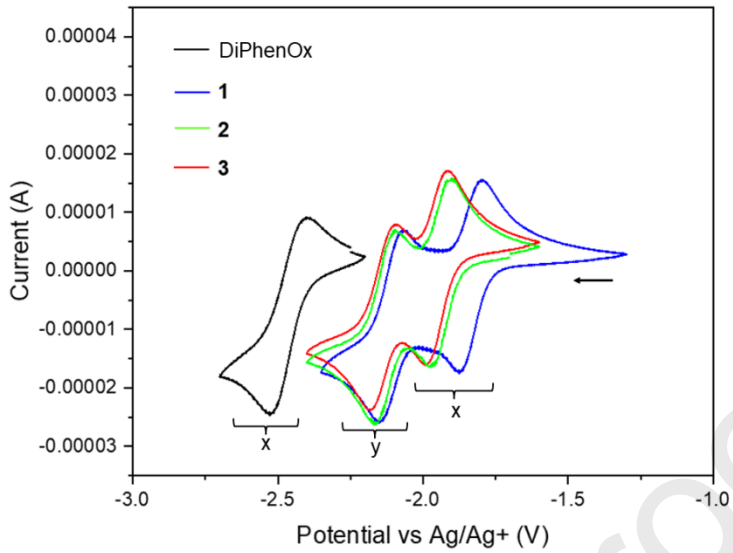

Figure 2. CV data of **1**, **2**, and **3** compared to DiPhenOx. All CV were collected reductively in MeCN at 1 mM concentration of the anolyte and 100 mM [TBA][PF_6] electrolyte with a scan rate of 100 mV/s and a $AgBF_4$ concentration of 25 mM for the Ag/Ag^+ reference electrode. The (x) refers to the first reductive event for each compound and (y) refers to the second reductive event for **1**, **2**, and **3**.

Table 1. Summary of CV data collected in MeCN with 1 mM of anolyte and 100 mM of [TBA][PF_6] at 100 mV/s. Scans were collected reductively as shown by the black arrow. Potentials are referenced to Ag/Ag^+ in MeCN. Current ratios i(c)/i(a) are shown in parenthesis.

$E_{1/2}$	DiPhenOx	**1**	**2**	**3**
1st reduction (x)	-2.46 (0.92)	-1.84 (0.94)	-1.94 (1.02)	-1.94 (0.92)
2nd reduction (y)	--	-2.12 (0.96)	-2.13 (0.89)	-2.14 (1.04)

*Kinetic parameters for **1**, **2**, and **3***

Rotating Disk Electrode (RDE) experiments were conducted on DiPhenOx, **1**, **2**, and **3** using a 3-electrode cell. The experiments were conducted in MeCN with 500 mM triethylammonium tetrafluoroborate ([TEA][BF_4]) as the supporting electrolyte. For compounds **1**, **2**, and **3**, each redox event was analyzed individually by identifying the inflection point between the two events on the RDE voltammogram to separate the data. By separating the events, we can find kinetic insight into why the first reduction (x) of **1**, **2**, and **3** exhibits improved performance

compared to DiPhenOx and compared to cycling over both events (x and y) of **1**, **2**, and **3**. The diffusion coefficients were calculated using the Levich equation and the standard rate constant and charge transfer coefficient were calculated with the Koutecký -Levich equation.[58]

From the RDE experiments, the diffusion coefficient of DiPhenOx was found to be 1.64x 10^{-5} cm^2 s^{-1}, while the average diffusion coefficient for **1**, **2**, and **3** was found to be 7.52 x $10^{-6\ 5}$ cm^2 s^{-1}, 7.48 x $10^{-6\ 5}$ cm^2 s^{-1}, and 7.61 x $10^{-6\ 5}$ cm^2 s^{-1} respectively (Table 2). The decrease in diffusion coefficient from DiPhenOx to **1**, **2**, and **3** can be explained by the increase in molar mass and change in solubility caused by the molecular modification, as discussed below. The standard rate constant (k^0) and the charge transfer coefficient (α) were calculated using the Koutecký - Levich equation. DiPhenOx and the first reduction (x) of **1**, **2**, and **3** had k^0 of similar magnitude while α exhibited some variation (Table 3). These k^0 values are larger than several common inorganic species such as V^{3+}/V^{2+} (4 x 10^{-7} cm s^{-1}) and Fe^{3+}/Fe^{2+},[59] but are on a similar order to or slightly better than several organic based redox active species.[60–62] The transfer coefficient for DiPhenOx and the first reduction (x) of **1** and **2** were within the acceptable range of the ideal value of 0.5. Conversely, **3**'s value of 0.89 deviates outside of this range. This is interesting as **3** performed better during bulk electrolysis testing (*vide infra*). The standard rate constant and charge transfer coefficient for the second reduction (y) reaction of **1**, **2**, and **3** differ greatly from DiPhenOx as well as their respective first reduction (x) reaction. The k^0 of the second reduction (y) reaction of **1**, **2**, and **3** dramatically increased while the charge transfer coefficient dropped below 0.2 for all derivatives. To fully understand the implications of these results requires more experiments planned for the future. In cases involving larger values of α, approaching or exceeding 1, it has been found that the limiting step is the adsorption of the molecule on to or off the electrode, rather than the transfer of electrons.[63,64] We have been unable to locate reports on the case of decreasing values of α. However, it can be speculated that the rate limiting step of the second reduction (y) reaction proceeds through a different mechanism as compared to DiPhenOx and the first reduction (x) reactions. This may contribute to the poor cyclability of the second reduction (y) reaction (see bulk electrolysis data and flow cell data). Future studies will focus on investigating these interesting kinetic parameters.

Table 2. Levich Analysis. Data collected in MeCN with 1 mM of anolyte and 500 mM of [TEA][BF_4] at 10 mV/s. Scans were collected reductively. Potentials are referenced to Ag/Ag^+ in MeCN.

Complex	1st Reduction (x) Diffusion Coefficient (D_o') [cm^2 s^{-1}]	2nd Reduction (y) Diffusion Coefficient (D_o') [cm^2 s^{-1}]	Average Diffusion Coefficient (D_o') [cm^2 s^{-1}]
DiPhenOx	1.64 x 10^{-5}	N/A	1.64 x 10^{-5}

1	8.27 x 10^{-6}	6.77 x 10^{-6}	7.52 x 10^{-6}
2	7.83 x 10^{-6}	7.13 x 10^{-6}	7.48 x 10^{-6}
3	7.90 x 10^{-6}	7.38 x 10^{-6}	7.61 x 10^{-6}

175

176

177 Table 3. Koutecký-Levich Analysis. Data collected in MeCN with 1 mM of anolyte and 500 mM
178 of [TEA][BF_4] supporting electrolyte at 10 mV/s. Scans were collected reductively. Potentials are
179 referenced to Ag/Ag^+ in MeCN.

Complex	1st Reduction (x) Standard Rate Constant (k^0) [cm s^{-1}]	2nd Reduction (y) Standard Rate Constant (k^0) [cm s^{-1}]	1st Reduction (x) Charge Transfer Coefficient (α)	2nd Reduction (y) Charge Transfer Coefficient (α)
DiPhenOx	0.093	N/A	0.66	N/A
1	0.046	0.255	0.57	0.096
2	0.084	0.376	0.68	0.19
3	0.069	0.357	0.89	0.080

180

181

182 *Bulk Electrolysis of **1**, **2**, and **3***

183 Bulk electrolysis experiments were conducted on DiPhenOx, **1**, **2**, and **3** using a symmetric
184 H-cell where each side contained an equimolar solution of the anolyte (Figures 3 and S 23-26). In
185 all cases, the modified compounds showed increased durability to cycling as compared to
186 DiPhenOx. Both **2** and **3** were extremely stable when the first reduction (x) potential was cycled,
187 with Coulombic efficiencies at 100% and no observable decrease in utilization values for charge
188 or discharge cycles. Compound **1** was less durable, with Coulombic efficiencies just below 100%

and a decrease of 0.22% and 0.49% in the utilization per cycle for charge and discharge respectively. However, **1** still showed a substantial improvement over DiPhenOx which exhibited a Coulombic efficiency of ~20% and greater than 80% loss in utilization for both the charge and discharge cycling by the termination of the experiment. When cycling the first and second reduction (x and y), **1**, **2**, and **3** all showed significant degradation over the course of 25 cycles, with the most dramatic decreases observed for **1**. Both **2** and **3** showed a ~50% decrease in utilization for the charge and discharge cycling in 25 cycles, while **1** had a >80% decrease in utilization within 10 cycles.

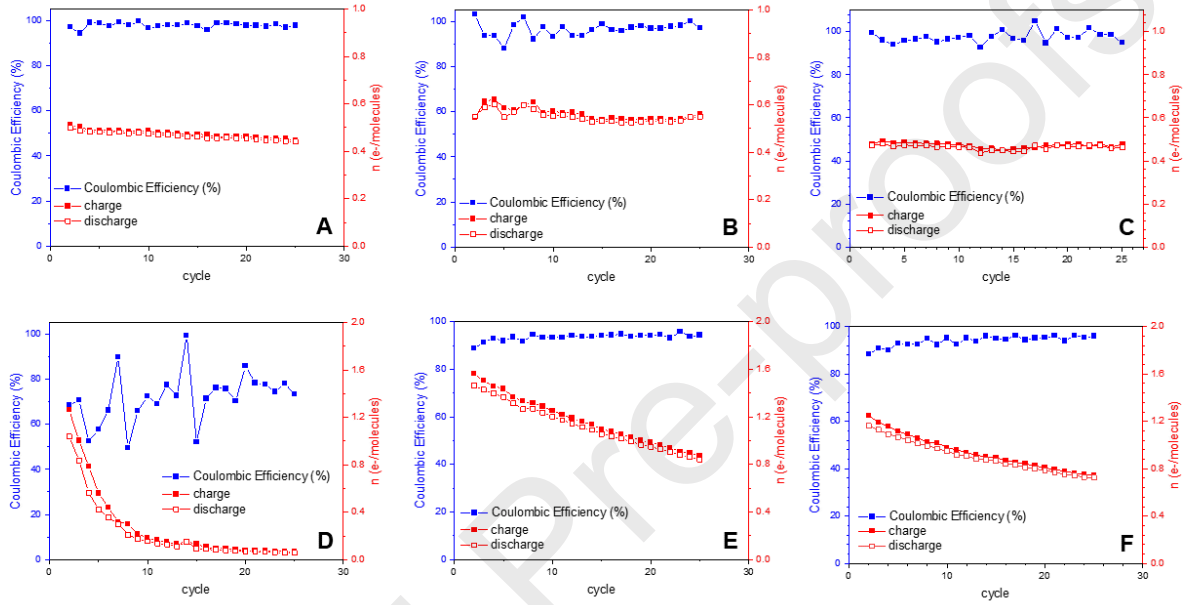

Figure 3. Bulk electrolysis data for **1** (A and D), **2** (B and E), and **3** (C and F) at 1 mM in MeCN with 100 mM supporting [TBA][PF_6] at 1 mA. A-C show cycling through the first redox event (x) (~50% SOC) while D-F show cycling through both redox events (x and y) (~100% SOC). The first cycle is not shown as it does not display representative charge and discharge behavior.

These data clearly demonstrate that while incorporating EWG's result in an additional reduction event as compared to the parent molecule, only the first of these reduction events (x) in **2** and **3** is stable to long-term cycling in a bulk electrolysis experiment. Therefore, the incorporation of ester moieties in **2** and **3** results in greater stabilizing effects for both reductions as compared to the incorporation of a cyano group in **1**. As evident from Figure 3 and S23-26, **3** shows good utilization for first reduction at ~50% state-of-charge (SOC). Therefore, **3** was further examined in flow cell and related discussions in next section.

Flow cell testing

Because bulk electrolysis cycling of compounds **2** and **3** revealed limited degradation when cycled at 50% SOC, we decided to further investigate these compounds in flow cell experiments. The flow cell cycling experiments utilizing **2** as the anolyte and ferrocene as the catholyte exhibited

unusual behavior. Despite increasing the SOC from 50% to 100%, we failed to observe a cumulative charge-dependent voltage profile. This failure to observe a charge or discharge voltage plateau is attributed to the electron transfer kinetics of the electrode for **2** (Figures S32-33). Additionally, **2** experienced a capacity loss of 27.1% over 200 cycles at 50% SOC, corresponding to a 0.136% capacity loss per cycle (Figure S32). This capacity loss exceeded that observed for **3** under identical conditions, where **3** exhibited a capacity loss of 9.13% over 200 cycles at 50% SOC, equating to a 0.045% capacity loss per cycle (Figure 4). Given the complex charge/discharge behavior displayed by **2** during flow cycling and its greater capacity loss compared to **3** under similar conditions, **3** was selected for subsequent flow cell cycling experiments.

Flow cell cycling to the first reduction (x) of compound **3** is shown in Figure 4. In order to evaluate the stability and cyclability of **3** in flow cell conditions, it was cycled versus known and highly reversibly ferrocene as catholyte until 50% SOC.[65] As demonstrated in Figure 5, the stability showed in the bulk electrolysis experiments is also reflected in the flow cell data. A stable Coulombic efficiency of ~96 % was obtained over 200 cycles (Figure 5b). Voltage and energy efficiencies also showed an excellent stability with values as high as ~91 % and ~88 % respectively among the best reported for non-aqueous RFBs.[26] The stable efficiency indicates the reversibility of **3** in flow battery cycling conditions. Capacity degradation poses a significant challenge for all RFBs, but it becomes particularly pronounced in asymmetric nonaqueous organic batteries. In these systems, the inability to regenerate organics and the need for extensive separation and purification exacerbates the problem. Consequently, it challenges the advantages of broader electrochemical stability window offered by nonaqueous solvents. Fortunately, compound **3** exhibits just 9.13% capacity loss, equivalent to 0.045% per cycle over 200 cycles. This impressive performance further solidifies its promise as a redox-active species for NRFBs. It should also be noted that the capacity fade indicates possible crossover and side reactions degrading redox active species in both cases it is irreversible for compound **3**.

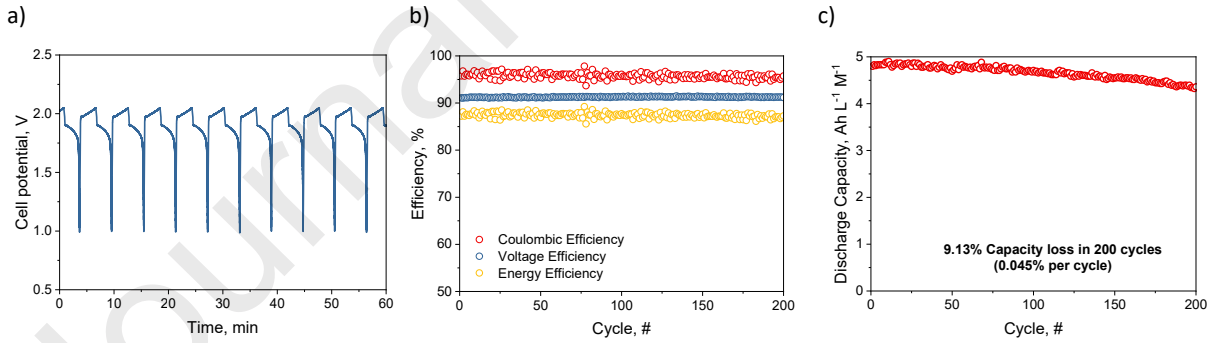

Figure 4. Cycling performance of NRFB using **3** as anolyte and ferrocene as catholyte. The cut-off voltage was 1.0 – 2.05 V (~ 50% SOC for the first reduction event). a) Potential vs. time plot; b) Coulombic, voltage and energy efficiencies; c) discharge capacity (2.5 mM compound **3** and 5 mM ferrocene in 250 mM [TEA][BF_4] used as anolyte and catholyte. The current density was 2.5 mA cm^{-2}).

Furthermore, cycling up to 100% SOC for **3** could enable non-aqueous RFBs to achieve higher energy density. Thus, compound **3** was cycled up to 2.10 V (~ 99% SOC) as illustrated in Figure 5. Cycling at a high SOC resulted in a slightly lower Coulombic efficiency, which gradually

increased over time from around 95% to about 98% (Figure 5b). Voltage and energy efficiencies remained mostly stable, with values around 90% for VE and 87% for EE, similar to those reported for 50% SOC. After 200 cycles, a total discharge capacity loss of 36.8% (0.184% per cycle) was observed. As expected, discharge capacity experienced significant degradation (Figure 5c) due to possibility of accessing second reduction event which was shown to be electrochemically irreversible.

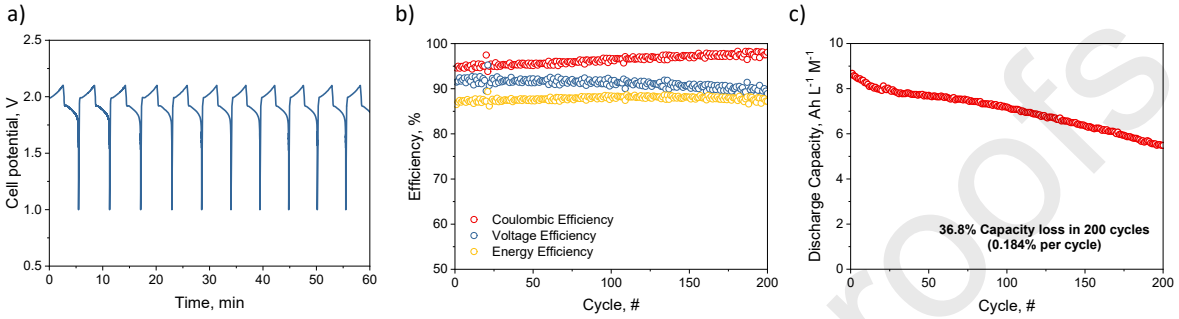

Figure 5. Cycling performance of NRFB using **3** as anolyte and ferrocene as catholyte. The cut-off voltage was 1.0 – 2.10 V (~ 100% SOC for the first reduction event). a) Potential vs. time plot; b) Coulombic, voltage and energy efficiencies; c) discharge capacity (2.5 mM compound **3** and 5 mM ferrocene in 250 mM [TEA][BF_4] used as anolyte and catholyte. The current density was 2.5 mA cm^{-2}).

The potential outcome of molecular engineering on DiPhenOx was enhancing its redox potential, cycling capability and solubility, potentially resulting in increased energy density in NRFBs. The DiPhenOx showed only one reduction event (Figure 2), and that did not cycle at 50% and 100% SOC (Figure S29 and S30), where the cell lost virtually all capacity in less than 25 cycles. These findings align well with the bulk electrolysis experiment. Cyano and ester derivatives of DiPhenOx have shown two distinct reduction events. Both of them are relatively more stable than the parent molecule, as evidenced from bulk electrolysis and flow cell cycling, which is a positive outcome of molecular engineering. Therefore, to assess the extent of reversibility of the second reduction (y) event in **3**, it was cycled between 1.0 V – 2.35 V, which corresponds to 50% SOC for the second reduction (Figure S28). The cell exhibited an initial coulombic efficiency of approximately 92%, which increased to about 96% in the first 50 cycles and stabilized. However, for the voltage and energy efficiencies, there was a considerable decrease from around 92% and 84% to 75% and 73%, respectively. This provides clear evidence of degradation *(vide infra*) of compound **3** when cycled for the second reduction event (Figure S34). Moreover, capacity retention was poor, and the cell lost 90.9% of discharge capacity in 200 cycles, which correlates well with the bulk electrolysis of compound **3**.

The relatively stable cycling of **3** at 50% SOC through the first negative wave makes it promising anolyte candidate for a > 3 V NRFB if coupled with appropriate and stable catholyte. Therefore, two literature reported catholytes, namely thianthrene ($E_{1/2}$: 0.92 V vs Ag/Ag^+) and 2,5-Di-tert-butyl-1,4-bis(2-methoxyethoxy)benzene (DBBB, $E_{1/2}$: 0.72 V vs Ag/Ag^+), were coupled with **3** and analyzed in NRFB cell.[46,66] The energy efficiencies and capacity decay rates for thianthrene and DBBB are presented in Figure 6 and S31, respectively. As expected, compound **3** exhibits good cycling behavior with both catholytes, with energy efficiencies hovering around

85% for thianthrene and approximately 90% for DBBB. It is worth noting that the capacity decay rates were 1.12% and 0.46% per cycle, respectively, for thianthrene and DBBB.

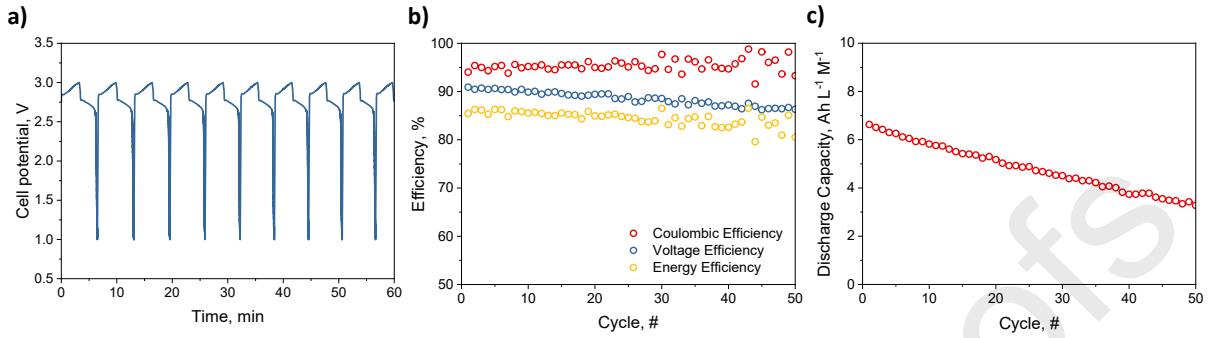

Figure 6. Cycling performance of NRFB using **3** as anolyte and thianthrene as catholyte. The cut-off voltage was 1.0 – 3.0 V (~ 50% SOC for the first reduction event). a) Potential vs. time plot; b) Coulombic, voltage and energy efficiencies; c) discharge capacity (2.5 mM compound **3** and 5 mM thianthrene in 250 mM [TEA][BF_4] used as anolyte and catholyte. The current density was 2.5 mA cm^{-2}).

Upon post-mortem analysis using CV of the electrolytes after the cycling test, it was found that the capacity decay was due to the chemical degradation of the anolytes (Figure S34). Cycling of **3** at 50% SOC for the first reduction event was the least detrimental, while running cycling tests at ~100% SOC was highly detrimental to **3**. However, electrolyte balance was not affected, as the ferrocene peak current at positive potential did not change significantly. In contrast, accessing the second reduction event resulted in the complete degradation of the anolyte, evident from the loss of peak current and redox features. It also affected the electrolyte balance, with ferrocene permeating into the anolyte from the catholyte, as indicated by increased peak currents in the anolyte. Similar degradation trends were observed when **3** was cycled with thianthrene and DBBB (Figure S 35). Thianthrene and DBBB themselves underwent degradation along with **3** at the reduction potential. Therefore, the relatively higher capacity decay rate is also attributed to the degradation of both thianthrene and DBBB when subjected to higher reduction potential in NRFBs. However, further study is needed to clearly identify the mode of degradation.

Effect of Modification on Solubility

While a clear improvement to the durability during cycling can be seen upon modification of DiPhenOx, this modification unfortunately also results in decreased solubility. While DiPhenOx has a reasonable solubility of 240 (30) mM in MeCN, **1**, **2**, and **3** have solubilities of 5.8(2) mM, 2.2(1) mM, and 2.7(3) mM in MeCN respectively (Tables S1-8 and Figures S13-16, see SI for experimental details). Although it is worth noting that the addition of an ether group in **3** results in a slight improvement in solubility over **2**, this increase is not nearly as large as the increases seen with other anolytes that incorporate PEG moieties.[39,52–55] Even **1**, the most soluble of the three derivatives, has extremely low saturation level. As such, extension of the aromatic system seems to both stabilize the charged form of the anolytes and decrease their solubility. Future studies on these anolytes should focus on modifying the stable **2** and **3** derivatives to increase solubility.

Potential directions include the addition of even longer PEG chains or the incorporation of charged groups such as sulfates or quaternary amines. Another possible research direction is into asymmetric DiPhenOx derivatives. Asymmetry in analytes is shown to increase solubility,[20,28] though these molecules can be synthetically challenging to make.

While the challenge of lower solubility must be addressed for **2** and **3** for their use as analytes in NRFBs, it is important to note that compound **3** demonstrates one of the lowest reduction voltages (-2.46 V vs Ag/Ag^{+}) among similar low-voltage carrier analytes, with their ability to undergo extensive cycling with minimal capacity loss (Table 4). Achieving >3 V NRFB is a significant accomplishment, making DiPhenOx derivatives a promising advancement in the molecular engineering of carrier molecules for NRFBs.

Table 4. A summary of the physical and electrochemical properties of analytes with negative potentials reported in literature:

Analyte	Potential (V vs. Ag/Ag+)	Solubility in MeCN (M)	Supporting Electrolyte in Flow Cell	Stability	Catholyte
DiPhenOx	-2.46	0.24(3)*	$TEABF_4$	not tested in a flow cell	N/A
1	-1.84 and -2.12	0.0058(2)	$TEABF_4$	not tested in a flow cell	N/A
2	-1.94 and -2.13	0.0022(1)	$TEABF_4$	capacity retention of 72% over 200 cycles	Ferrocene
3	-1.94 and -2.14	0.0027(3)	$TEABF_4$	capacity retention of 90.87% over 200 cycles	Ferrocene
9-fluorenone[1]	-1.64	2	TEATFSI	capacity retention of 50% over 50 cycles	2,5-di-tert-butyl-1-methoxy-4-[2′-methoxyethoxy]benzene (DBMMB)
benzophenone[2]	-2.16	4.3	$TEAPF_6$	stable over 7 cycles	tetramethyl-1-piperidinyloxy (TEMPO)
4,4'-dimethylbenzophenone[3]	-2.26	0.8	$TEAPF_6$	Average Coulombic efficiency of 72% over 95 cycles	2,5-Di-tert-butyl-1,4-dimethoxybenzene (DBB)
4,4'-dimethoxybenzophenone[3]	-2.37	0.09	$TEAPF_6$	not tested in a flow cell	N/A
2-methylbenzophenone[4]	-2.26	miscible	$TEAPF_6$	Average Coulombic efficiency of 95% over 50 cycles	2,5-di-tert-butyl-1-methoxy-4-[2′-methoxyethoxy]benzene (DBMMB)
3-methylbenzophenone[5]	-2.18	miscible	$TEAPF_6$	stable over 30 cycles	1,4-di-tert-butyl-2-methoxy-5-(2-methoxyethoxy)benzene (DBMMB)
azobenzene[6]	-1.69	0.7	$TEAPF_6$	Capacity retention of 70.8% over 80 cycles	PEG3-phenothiazine

*standard deviation given in parentheses; [1][67]; [2][68]; [3][69]; [4][70]; [5][71]; [6][72]

CONCLUSIONS

While initial CV experiments suggested that DiPhenOx should perform well as an analyte in a NRFB, testing in bulk electrolysis and flow cell experiments demonstrated that this molecule is not durable to cycling. We employed a molecular engineering approach to modify the parent DiPhenOx in order to stabilize the charged states of the molecule. Our findings indicate that incorporating ester groups in the para position of the arene rings resulted in a highly durable analyte at the expense of solubility. The addition of a cyano group resulted in a DiPhenOx

derivative that was more stable to cycling than DiPhenOx itself but showed clear degradation during cycling experiments and low solubility. Moreover, we showed that coupling the ester derivatives with high potential-containing positive electrolytes resulted in >3 V NRFBs. Future work will focus on increasing the solubility and electrochemical stability of compounds **2** and **3**.

ASSOCIATED CONTENT

Supporting Information. Additional description of general methods, synthesis, characterization, spectroscopy, solubility, and electrochemical measurements.

Author Contributions

The manuscript was written through contributions of all authors. All authors have given approval to the final version of the manuscript.

ACKNOWLEDGMENT

This work was supported by the Laboratory Directed Research and Development (LDRD) program of Los Alamos National Laboratory (LANL) under project number 20210680ECR. Los Alamos National Laboratory is operated by Triad, LLC, for the National Nuclear Security Administration of the U.S. Department of Energy (Contract No. 89233218NCA000001). Two authors are supported by the TAMU-LANL Collaborative Research Program.

REFERENCES

[1] O. Comstock, Today in Energy EIA expects renewables to account for 22 % of U . S . electricity generation in 2022, August 16 (2022). https://www.eia.gov/todayinenergy/detail.php?id=53459.

[2] P. Leung, X. Li, C. Ponce De León, L. Berlouis, C.T.J. Low, F.C. Walsh, Progress in redox flow batteries, remaining challenges and their applications in energy storage, RSC Adv 2 (2012) 10125–10156. https://doi.org/10.1039/c2ra21342g.

[3] Water Power Technologies Office, Pumped Storage Hydropower | Department of Energy, (n.d.). https://www.energy.gov/eere/water/pumped-storage-hydropower (accessed March 17, 2024).

[4] R. Shan, J. Reagan, S. Castellanos, S. Kurtz, N. Kittner, Evaluating emerging long-duration energy storage technologies, Renewable and Sustainable Energy Reviews 159 (2022) 112240. https://doi.org/10.1016/j.rser.2022.112240.

[5] R. Cairns, This giant “water battery” under the Alps could be a game- changer for renewable energy in Europe, CNN (2022) Accessed on August 19, 2022. https://www.cnn.com/2022/08/01/world/water-battery-switzerland-renewable-energy-climate-scn-hnk-spc-intl/index.html.

[6] R. Uria-Martinez, M. Johnson, S. Rui, U.S Hydropower Market Report - Water power technologies office, Office of Energy Efficiency & Renewable Energy (2021). https://doi.org/10.2172/1763453.

[7] M. Mann, V. Putsche, B. Shrager, Grid energy storage supply chain deep dive assessment, U. S. Department of Energy Response to Executive Order 14017, "America's Supply Chains" (2022) 1–58. https://doi.org/10.2172/1871557.

[8] J.P. Hoffstaedt, D.P.K. Truijen, J. Fahlbeck, L.H.A. Gans, M. Qudaih, A.J. Laguna, J.D.M. De Kooning, K. Stockman, H. Nilsson, P.T. Storli, B. Engel, M. Marence, J.D. Bricker, Low-head pumped hydro storage: A review of applicable technologies for design, grid integration, control and modelling, Renewable and Sustainable Energy Reviews 158 (2022) 112119. https://doi.org/10.1016/j.rser.2022.112119.

[9] M.R.N. Vilanova, A.T. Flores, J.A.P. Balestieri, Pumped hydro storage plants: a review, Journal of the Brazilian Society of Mechanical Sciences and Engineering 42 (2020) 1–14. https://doi.org/10.1007/s40430-020-02505-0.

[10] G. Ardizzon, G. Cavazzini, G. Pavesi, A new generation of small hydro and pumped-hydro power plants: Advances and future challenges, Renewable and Sustainable Energy Reviews 31 (2014) 746–761. https://doi.org/10.1016/j.rser.2013.12.043.

[11] R. Chen, D. Bresser, M. Saraf, P. Gerlach, A. Balducci, S. Kunz, D. Schröder, S. Passerini, J. Chen, A Comparative Review of Electrolytes for Organic-Material-Based Energy-Storage Devices Employing Solid Electrodes and Redox Fluids, ChemSusChem 13 (2020) 2205–2219. https://doi.org/10.1002/cssc.201903382.

[12] T.C. Palmer, A. Beamer, T. Pitt, I.A. Popov, C.X. Cammack, H.D. Pratt, T.M. Anderson, E.R. Batista, P. Yang, B.L. Davis, A Comparative Review of Metal-Based Charge Carriers in Nonaqueous Flow Batteries, ChemSusChem 14 (2021) 1214–1228. https://doi.org/10.1002/cssc.202002354.

[13] G.L. Soloveichik, Flow Batteries: Current Status and Trends, Chem Rev 115 (2015) 11533–11558. https://doi.org/10.1021/cr500720t.

[14] L. Li, S. Kim, W. Wang, M. Vijayakumar, Z. Nie, B. Chen, J. Zhang, G. Xia, J. Hu, G. Graff, J. Liu, Z. Yang, A stable vanadium redox-flow battery with high energy density for large-scale energy storage, Adv Energy Mater 1 (2011) 394–400. https://doi.org/10.1002/aenm.201100008.

[15] V. Murugesan, Z. Nie, X. Zhang, P. Gao, Z. Zhu, Q. Huang, L. Yan, D. Reed, W. Wang, Accelerated design of vanadium redox flow battery electrolytes through tunable solvation chemistry, Cell Rep Phys Sci 2 (2021) 100323. https://doi.org/10.1016/j.xcrp.2021.100323.

[16] Z. Huang, A. Mu, L. Wu, B. Yang, Y. Qian, J. Wang, Comprehensive Analysis of Critical Issues in All-Vanadium Redox Flow Battery, ACS Sustain Chem Eng 10 (2022) 7786–7810. https://doi.org/10.1021/acssuschemeng.2c01372.

[17] K.J. Kim, M.S. Park, Y.J. Kim, J.H. Kim, S.X. Dou, M. Skyllas-Kazacos, A technology review of electrodes and reaction mechanisms in vanadium redox flow batteries, J Mater Chem A Mater 3 (2015) 16913–16933. https://doi.org/10.1039/c5ta02613j.

[18] J.D. Saraidaridis, C.W. Monroe, Nonaqueous vanadium disproportionation fl ow batteries with porous separators cycle stably and tolerate high current density, Journal of Power Souces 412 (2019) 384–390. https://doi.org/10.1016/j.jpowsour.2018.11.058.

[19] B. Zhang, B.R. Schrage, A. Frkonja-Kuczin, S. Gaire, I.A. Popov, C.J. Ziegler, A. Boika, Zwitterionic Ferrocenes: An Approach for Redox Flow Battery (RFB) Catholytes, Inorg Chem 61 (2022) 8117–8120. https://doi.org/10.1021/acs.inorgchem.2c00722.

[20] X. Li, P. Gao, Y.Y. Lai, J.D. Bazak, A. Hollas, H.Y. Lin, V. Murugesan, S. Zhang, C.F. Cheng, W.Y. Tung, Y.T. Lai, R. Feng, J. Wang, C.L. Wang, W. Wang, Y. Zhu, Symmetry-breaking design of an organic iron complex catholyte for a long cyclability aqueous organic redox flow battery, Nat Energy 6 (2021) 873–881. https://doi.org/10.1038/s41560-021-00879-6.

[21] Y. Zhen, C. Zhang, J. Yuan, Y. Zhao, Y. Li, A high-performance all-iron non-aqueous redox flow battery, Journal of Power Souces 445 (2020) 1–8.

[22] T.N. Pham-Truong, Q. Wang, J. Ghilane, H. Randriamahazaka, Recent Advances in the Development of Organic and Organometallic Redox Shuttles for Lithium-Ion Redox Flow Batteries, ChemSusChem 13 (2020) 2142–2159. https://doi.org/10.1002/cssc.201903379.

[23] I.A. Popov, N. Mehio, T. Chu, B.L. Davis, R. Mukundan, P. Yang, E.R. Batista, Impact of Ligand Substitutions on Multielectron Redox Properties of Fe Complexes Supported by Nitrogenous Chelates, ACS Omega 3 (2018) 14766–14778. https://doi.org/10.1021/acsomega.8b01921.

[24] X. Wei, L. Cosimbescu, W. Xu, J.Z. Hu, M. Vijayakumar, J. Feng, M.Y. Hu, X. Deng, J. Xiao, J. Liu, V. Sprenkle, W. Wang, Towards high-performance nonaqueous redox flow electrolyte via ionic modification of active species, Adv Energy Mater 5 (2015) 1–7. https://doi.org/10.1002/aenm.201400678.

[25] Z. Zhao, B. Zhang, B.R. Schrage, C.J. Ziegler, A. Boika, Investigations into aqueous redox flow batteries based on ferrocene bisulfonate, ACS Appl Energy Mater 3 (2020) 10270–10277. https://doi.org/10.1021/acsaem.0c02259.

[26] S. Sharma, G.A. Andrade, S. Maurya, I.A. Popov, E.R. Batista, B.L. Davis, R. Mukundan, N.C. Smythe, A.M. Tondreau, P. Yang, J.C. Gordon, Iron-iminopyridine complexes as charge carriers for non-aqueous redox flow battery applications, Energy Storage Mater 37 (2021) 576–586. https://doi.org/10.1016/j.ensm.2021.01.035.

[27] A.W. Lantz, S.A. Shavalier, W. Schroeder, P.G. Rasmussen, Evaluation of an Aqueous Biphenol- and Anthraquinone-Based Electrolyte Redox Flow Battery, Applied Energy Materials 2 (2019) 7893–7902. https://doi.org/10.1021/acsaem.9b01381.

[28] W. Wang, W. Xu, L. Cosimbescu, D. Choi, L. Li, Z. Yang, Anthraquinone with tailored structure for a nonaqueous metal-organic redox flow batter, Chemical Communications 48 (2012) 6669–6671. https://doi.org/10.1039/c2cc32466k.

[29] Y. Zhen, C. Zhang, J. Yuan, Y. Li, Anthraquinone-based electroactive ionic species as stable multi-redox anode active materials for high-performance nonaqueous redox flow batteries, J Mater Chem A Mater 9 (2021) 22056–22063. https://doi.org/10.1039/d1ta04546f.

[30] Y. Zhen, C. Zhang, Y. Li, Coupling Tetraalkylammonium and Ethylene Glycol Ether Side Chain To Enable Highly Soluble Anthraquinone-Based Ionic Species for Nonaqueous Redox Flow Battery, ACS Appl Mater Interfaces 14 (2022) 17369–17377. https://doi.org/10.1021/acsami.2c01569.

[31] Z. Li, T. Jiang, M. Ali, C. Wu, W. Chen, Recent Progress in Organic Species for Redox Flow Batteries, Energy Storage Mater 50 (2022) 105–138. https://doi.org/10.1016/j.ensm.2022.04.038.

[32] M. Wu, M. Bahari, E.M. Fell, R.G. Gordon, M.J. Aziz, High-performance anthraquinone with potentially low cost for aqueous redox flow batteries, J Mater Chem A Mater 9 (2021) 26709–26716. https://doi.org/10.1039/d1ta08900e.

[33] E.F. Kerr, Z. Tang, T.Y. George, S. Jin, E.M. Fell, K. Amini, Y. Jing, M. Wu, R.G. Gordon, M.J. Aziz, High Energy Density Aqueous Flow Battery Utilizing Extremely Stable, Branching-Induced High-Solubility Anthraquinone near Neutral pH, ACS Energy Lett (2022) 600–607. https://doi.org/10.1021/acsenergylett.2c01691.

[34] R. Feng, Z. Xin, V. Murugesan, A. Hollas, Y. Chen, Y. Shao, E. Walter, N.P.N. Wellala, L. Yan, K.M. Rosso, W. Wang, Reversible ketone hydrogenation and dehydrogenation for aqueous organic redox flow batteries, Science (1979) 3722 (2021) 836–840. https://doi.org/10.1126/science.abd9795.

[35] J. Rodriguez, C. Niemet, L.D. Pozzo, Fluorenone Based Anolyte for an Aqueous Organic Redox-Flow Battery, ECS Meeting Abstracts MA2019-01 (2019) 453–453. https://doi.org/10.1149/ma2019-01/3/453.

[36] D.P. Leonard, Z. Wei, G. Chen, F. Du, X. Ji, Water-in-Salt Electrolyte for Potassium-Ion Batteries, ACS Energy Lett 3 (2018) 373–374. https://doi.org/10.1021/acsenergylett.8b00009.

[37] M.V. Holland-Cunz, F. Cording, J. Friedl, U. Stimming, Redox flow batteries—Concepts and chemistries for cost-effective energy storage, Frontiers in Energy 12 (2018) 198–224. https://doi.org/10.1007/s11708-018-0552-4.

[38] R.M. Darling, K.G. Gallagher, J.A. Kowalski, S. Ha, F.R. Brushett, Pathways to low-cost electrochemical energy storage: A comparison of aqueous and nonaqueous flow batteries, Energy Environ Sci 7 (2014) 3459–3477. https://doi.org/10.1039/c4ee02158d.

[39] P.J. Cabrera, X. Yang, J.A. Suttil, K.L. Hawthorne, R.E.M. Brooner, M.S. Sanford, L.T. Thompson, Complexes containing redox noninnocent ligands for symmetric, multielectron transfer nonaqueous redox flow batteries, Journal of Physical Chemistry C 119 (2015) 15882–15889. https://doi.org/10.1021/acs.jpcc.5b03582.

[40] J.A. Suttil, J.F. Kucharyson, P.J. Cabrera, B.R. James, R.F. Savinell, M.S. Sanford, L.T. Thompson, Metal acetylacetonate complexes for high energy density non-aqueous redox flow batteries, Journal of Material Chemistry A 3 (2015) 7929–7938. https://doi.org/10.1039/c4ta06622g.

[41] T. Chu, I.A. Popov, G.A. Andrade, S. Maurya, P. Yang, E.R. Batista, B.L. Scott, R. Mukundan, B.L. Davis, Linked Picolinamide Nickel Complexes as Redox Carriers for Nonaqueous Flow Batteries, ChemSusChem 12 (2019) 1304–1309. https://doi.org/10.1002/cssc.201802985.

[42] G.A. Andrade, I.A. Popov, C.R. Federico, P. Yang, E.R. Batista, R. Mukundan, B.L. Davis, Expanding the potential of redox carriers for flow battery applications, J Mater Chem A Mater 8 (2020) 17808–17816. https://doi.org/10.1039/d0ta04511j.

[43] K.A. Jesse, S.D. Abad, C. Studvick, G.A. Andrade, S. Maurya, B.L. Scott, R. Mukundan, I.A. Popov, B.L. Davis, Impact of Pendent Ammonium Groups on Solubility and Cycling Charge Carrier Performance in Nonaqueous Redox Flow Batteries, Inorg Chem 62 (2023). https://doi.org/10.1021/acs.inorgchem.3c02396.

[44] J. Luo, B. Hu, M. Hu, Y. Zhao, T.L. Liu, Status and Prospects of Organic Redox Flow Batteries toward Sustainable Energy Storage, ACS Energy Lett 4 (2019) 2220–2240. https://doi.org/10.1021/acsenergylett.9b01332.

[45] J.M. Cameron, C. Holc, A.J. Kibler, C.L. Peake, D.A. Walsh, G.N. Newton, L.R. Johnson, Molecular redox species for next-generation batteries, Chem Soc Rev 50 (2021) 5863–5883. https://doi.org/10.1039/d0cs01507e.

[46] C.P. Keszthelyi, H. Tachikawa, A.J. Bard, Electrogenerated Chemiluminescence. VIII. The Thianthrene-2,5-Diphenyl-1,3,4-oxadiaxole System. A Mixed Energy-Sufficient System, J Am Chem Soc 209 (1972) 1522–1527. https://doi.org/10.1021/ja00760a014.

[47] N.G. Connelly, W.E. Geiger, Chemical Redox Agents for Organometallic Chemistry, Chem Rev 96 (1996) 877–910. https://doi.org/https://doi.org/10.1021/cr940053x.

[48] M.R. Gerhardt, L. Tong, R. Gómez-Bombarelli, Q. Chen, M.P. Marshak, C.J. Galvin, A. Aspuru-Guzik, R.G. Gordon, M.J. Aziz, Anthraquinone Derivatives in Aqueous Flow Batteries, Adv Energy Mater 7 (2017). https://doi.org/10.1002/aenm.201601488.

[49] J. Zhang, J. Huang, L.A. Robertson, R.S. Assary, I.A. Shkrob, L. Zhang, Elucidating Factors Controlling Long-Term Stability of Radical Anions for Negative Charge Storage in Nonaqueous Redox Flow Batteries, Journal of Physical Chemistry C 122 (2018) 8116–8127. https://doi.org/10.1021/acs.jpcc.8b01434.

[50] B.P. Das, R.A. Wallace, D.W. Boykin, Synthesis and Antitrypanosomal Activity of some Bis(4-Guanylphenyl) Five- and Six-Membered Ring Heterocycles, J Med Chem 23 (1980) 578–581. https://doi.org/10.1021/jm00179a022.

[51] J. Noack, N. Roznyatovskaya, T. Herr, P. Fischer, The Chemistry of Redox-Flow Batteries, Angewandte Chemie - International Edition 54 (2015) 9776–9809. https://doi.org/10.1002/anie.201410823.

[52] P.J. Cabrera, X. Yang, J.A. Suttil, R.E.M. Brooner, L.T. Thompson, M.S. Sanford, Evaluation of Tris-Bipyridine Chromium Complexes for Flow Battery Applications: Impact of Bipyridine Ligand Structure on Solubility and Electrochemistry, Inorg Chem 54 (2015) 10214–10223. https://doi.org/10.1021/acs.inorgchem.5b01328.

[53] M. V. Makarova, A. V. Akkuratov, M.E. Sideltsev, K.J. Stevenson, E.I. Romadina, Novel Ethylene Glycol Substituted Benzoxadiazole and Benzothiadiazole as Anolytes for Nonaqueous Organic Redox Flow Batteries, ChemElectroChem 9 (2022) 1–7. https://doi.org/10.1002/celc.202200483.

[54] E.I. Romadina, I.A. Volodin, K.J. Stevenson, P.A. Troshin, New highly soluble triarylamine-based materials as promising catholytes for redox flow batteries, J Mater Chem A Mater 9 (2021) 8303–8307. https://doi.org/10.1039/d0ta11860e.

[55] E.I. Romadina, D.S. Komarov, K.J. Stevenson, P.A. Troshin, New phenazine based anolyte material for high voltage organic redox flow batteries, Chemical Communications 57 (2021) 2986–2989. https://doi.org/10.1039/d0cc07951k.

[56] H. Cruz, N. Jordão, P. Amorim, M. Dionísio, L.C. Branco, Deep Eutectic Solvents as Suitable Electrolytes for Electrochromic Devices, ACS Sustain Chem Eng 6 (2018) 2240–2249. https://doi.org/10.1021/acssuschemeng.7b03684.

[57] B. Chen, S. Mitchell, N. Sinclair, J. Wainright, E. Pentzer, B. Gurkan, Feasibility of TEMPO-functionalized imidazolium, ammonium and pyridinium salts as redox-active carriers in ethaline deep eutectic solvent for energy storage, Mol Syst Des Eng 5 (2020) 1147–1157. https://doi.org/10.1039/d0me00038h.

[58] H. Wang, S.Y. Sayed, E.J. Luber, B.C. Olsen, S.M. Shirurkar, S. Venkatakrishnan, U.M. Tefashe, A.K. Farquhar, E.S. Smotkin, R.L. McCreery, J.M. Buriak, Redox Flow Batteries: How to Determine Electrochemical Kinetic Parameters, ACS Nano 14 (2020) 2575–2584. https://doi.org/10.1021/acsnano.0c01281.

[59] A.Z. Weber, M.M. Mench, J.P. Meyers, P.N. Ross, J.T. Gostick, Q. Liu, Redox flow batteries: A review, J Appl Electrochem 41 (2011) 1137–1164. https://doi.org/10.1007/s10800-011-0348-2.

[60] T. Hagemann, J. Winsberg, A. Wild, U.S. Schubert, Synthesis and Electrochemical Study of a TCAA Derivative – A potential bipolar redox-active material, Electrochim Acta 228 (2017) 494–502. https://doi.org/10.1016/j.electacta.2017.01.055.

[61] B. Huskinson, M.P. Marshak, C. Suh, S. Er, M.R. Gerhardt, C.J. Galvin, X. Chen, A. Aspuru-Guzik, R.G. Gordon, M.J. Aziz, A metal-free organic-inorganic aqueous flow battery, Nature 505 (2014) 195–198. https://doi.org/10.1038/nature12909.

[62] T. Janoschka, N. Martin, M.D. Hager, U.S. Schubert, An Aqueous Redox-Flow Battery with High Capacity and Power: The TEMPTMA/MV System, Angewandte Chemie - International Edition 55 (2016) 14427–14430. https://doi.org/10.1002/anie.201606472.

[63] N.A. Shaheen, W. Dean, D. Penley, B. Kersten, J. Rintamaki, M.B. Vukmirovic, B.E. Gurkan, R. Akolkar, Electro–Oxidation of Nitroxide Radicals: Adsorption–Mediated Charge Transfer Probed Using SERS and Potentiometry, J Electrochem Soc 169 (2022) 053511. https://doi.org/10.1149/1945-7111/ac7082.

[64] R. Guidelli, R.G. Compton, J.M. Feliu, E. Gileadi, J. Lipkowski, W. Schmickler, S. Trasatti, Defining the transfer coefficient in electrochemistry: An assessment (IUPAC Technical Report), Pure and Applied Chemistry 86 (2014) 245–258. https://doi.org/10.1515/pac-2014-5026.

[65] Y. Ding, Y. Zhao, Y. Li, J.B. Goodenough, G. Yu, A high-performance all-metallocene-based, non-aqueous redox flow battery, Energy Environ Sci 10 (2017) 491–497. https://doi.org/10.1039/c6ee02057g.

[66] F.R. Brushett, J.T. Vaughey, A.N. Jansen, An all-organic non-aqueous lithium-ion redox flow battery, Adv Energy Mater 2 (2012) 1390–1396. https://doi.org/10.1002/aenm.201200322.

[67] X. Wei, W. Xu, J. Huang, L. Zhang, E. Walter, C. Lawrence, M. Vijayakumar, W.A. Henderson, T. Liu, L. Cosimbescu, B. Li, V. Sprenkle, W. Wang, Radical Compatibility with Nonaqueous Electrolytes and Its Impact on an All-Organic Redox Flow Battery, Angewandte Chemie 127 (2015) 8808–8811. https://doi.org/10.1002/ange.201501443.

[68] X. Xing, Y. Huo, X. Wang, Y. Zhao, Y. Li, A benzophenone-based anolyte for high energy density all-organic redox flow battery, Int J Hydrogen Energy 42 (2017) 17488–17494. https://doi.org/10.1016/j.ijhydene.2017.03.034.

[69] Y. Huo, X. Xing, C. Zhang, X. Wang, Y. Li, An all organic redox flow battery with high cell voltage, RSC Adv 9 (2019) 13128–13132. https://doi.org/10.1039/c9ra01514k.

[70] X. Xing, Q. Liu, W. Xu, W. Liang, J. Liu, B. Wang, J.P. Lemmon, All-Liquid Electroactive Materials for High Energy Density Organic Flow Battery, ACS Appl Energy Mater 2 (2019) 2364–2369. https://doi.org/10.1021/acsaem.8b01874.

[71] X. Xing, Q. Liu, B. Wang, J.P. Lemmon, W.Q. Xu, A low potential solvent-miscible 3-methylbenzophenone anolyte material for high voltage and energy density all-organic flow battery, J Power Sources 445 (2020). https://doi.org/10.1016/j.jpowsour.2019.227330.

[72] X. Wang, J. Chai, A. Lashgari, J.J. Jiang, Azobenzene-Based Low-Potential Anolyte for Nonaqueous Organic Redox Flow Batteries, ChemElectroChem 8 (2021) 83–89. https://doi.org/10.1002/celc.202001035.

- Stable derivatives of DiPhenOx are synthesized and characterized as anolytes.
- Cyano and ester groups improve electrochemical stability of parent molecule.
- Adding an ester group does not always increase solubility in non-aqueous solutions.
- DiPhenOx derivatives paired with catholytes enable >3 V non-aqueous redox flow battery.